TECHNICAL REPORT ARTSD-TR-81002

SIX-DEGREE-OF-FREEDOM (6-DOF) SIMULATOR FOR WEAPON TESTING

DONALD E. FRERICKS
ROBERT J. RADKIEWICZ

MARCH 1982

US ARMY ARMAMENT RESEARCH AND DEVELOPMENT COMMAND
TECHNICAL SUPPORT DIRECTORATE
DOVER, NEW JERSEY

The views, opinions, and/or findings contained in this report are those of the author and should not be construed as an official Department of the Army position, policy or decision, unless so designated by other documentation.

Destroy this report when no longer needed. Do not return to the originator.

The citation in this report of the names of commercial firms or commercially available products or services does not constitute official endorsement or approval of such commercial firms, products, or services by the US Government.

REPORT DOCUMENTATION PAGE

READ INSTRUCTIONS BEFORE COMPLETING FORM

1. REPORT NUMBER: Technical Report ARTSD-TR-81002
2. GOVT ACCESSION NO.:
3. RECIPIENT'S CATALOG NUMBER:

4. TITLE (and Subtitle): SIX-DEGREE-OF-FREEDOM (6-DOF) SIMULATOR FOR WEAPON TESTING

5. TYPE OF REPORT & PERIOD COVERED: Final

6. PERFORMING ORG. REPORT NUMBER:

7. AUTHOR(s):
Donald E. Frericks
Robert J. Radkiewicz

8. CONTRACT OR GRANT NUMBER(s):

9. PERFORMING ORGANIZATION NAME AND ADDRESS:
ARRADCOM, TSD
Ware Simulation Section (DRDAR-TSE-SW)
Rock Island, IL 61299

10. PROGRAM ELEMENT, PROJECT, TASK AREA & WORK UNIT NUMBERS:
AMS Code
3297.06.7313 (cont)

11. CONTROLLING OFFICE NAME AND ADDRESS:
ARRADCOM, TSD
STINFO Div (DRDAR-TSS)
Dover, NJ 07801

12. REPORT DATE: March 1982

13. NUMBER OF PAGES: 39

14. MONITORING AGENCY NAME & ADDRESS(if different from Controlling Office):
ARRADCOM, TSD
Test and Instrumentation Div (DRDAR-TSE-S)
Dover, NJ 07801

15. SECURITY CLASS. (of this report): Unclassified

15a. DECLASSIFICATION/DOWNGRADING SCHEDULE:

16. DISTRIBUTION STATEMENT (of this Report)
Approved for public release; distribution unlimited.

17. DISTRIBUTION STATEMENT (of the abstract entered in Block 20, if different from Report)

18. SUPPLEMENTARY NOTES The detailed design study performed by the Franklin Institute Research Laboratory for the simulator provides more complete details and is published separately as a special publication (ARTSD-SP-81001).

The mechanical and electrical design drawings for the 6-DOF simulator are on file at the Ware Simulation Section.

19. KEY WORDS (Continue on reverse side if necessary and identify by block number)

Control system	Six degrees-of-freedom
Hydraulics	Spring rate
Pitch	Vibration
Simulator	Weapons
Yaw	

20. ABSTRACT (Continue on reverse side if necessary and identify by block number)

A six-degree-of-freedom (6-DOF) simulator has been constructed and implemented as a test bed for military vehicles or individual weapon systems. These weapon systems are either attached directly to the simulator or connected to vehicle sections suspended from it. Simulation includes firing and response to firing loads using appropriate conversion and movement which parallels weapon firing in the field. While firing, the weapon system can be moved in either simple harmonic motion driven by a signal generator or complex motion obtained from a field tape operated by a digital computer. Vibrations typical (cont)

Block 10 (cont)

Projects no. 6737313, 6747313, 6767313, and 6777313.

Block 20 (cont)

of the field environment are input through the actuator.

CONTENTS

TABLES

FIGURES

INTRODUCTION

Background

An activated six-degree-of-freedom (6-DOF) simulator has been designed, constructed, and tested under several Production Engineering Measures (PEM) projects extending over many years. The project numbers are listed on the preceding Report Documentation Page for reference. This report outlines accomplishments achieved under these projects and provides the capabilities of the activated 6-DOF simulator.[1]

The 6-DOF simulator is a test bed to which sections of military vehicles or individual weapon systems are attached. The weapon systems, whether attached either directly to the simulator or attached to vehicle sections that are suspended from the simulator, are fired and the simulator responds to the firing loads in the three translational and the three rotational degrees of freedom, which parallels weapon firing in the field instead of in a laboratory. The weapon system may be simultaneously moved in either yaw or pitch motion. The motions may be simple harmonic motion driven by a signal generator or complex motion obtained from a field tape driven by a digital computer. Vibrations typical of the desired field environments can be input through the hydraulic actuator system. The simulator is thus capable of providing a more realistic test environment in terms of the mechanical characteristics, typical vibrations, and motions than has previously been possible.

Classical methods for the acceptance testing of automatic weapons usually include a function-firing test under a single specified mounting condition. Such tests are a go or no-go inspection at a single point in the spectrum of dynamic conditions under which weapons are expected to operate in the field. This type of testing is adequate for low rate-of-fire weapons of the past but lacks the capability for discriminating between reliable and unreliable weapons of the high rate-of-fire type that are intended for installation on highly flexible, moving, and vibrating gun platforms. A truly definitive acceptance test must include active simulation of the structural vibrations induced by vehicle motion during the course of testing.

---

[1] The detailed design study performed by the Franklin Institute Research Laboratories (FIRL) for the simulator provides more complete details of the overall system and is published separately as a corresponding special publication (ARTSD-SP-81001).

Advantages of Laboratory Testing

Both in cost savings and technical data obtained, the laboratory testing of weapon systems offers significant advantages over field testing. These advantages include: (1) repeatability of test setups, (2) freedom from requalification of vehicle after making structural changes, (3) ability to test several systems under identical conditions, thus enabling an unbiased evaluation of competing weapons, (4) considerable increase in the type and quantity of data gathered, (5) test schedules not affected by adverse weather conditions, and (6) reduction in the number of test and safety personnel.

This report explains the modifications that were made to the simulator in converting from passive to active which makes it capable of providing the dynamic environment described in the previous paragraphs. These modifications provide the fire-on-the-move capability required for simultaneous two-axis evaluation of new weapons with stabilization systems.

The objective of PEM Project 6737313 was to improve the existing test procedures for production and acceptance testing of weapon systems. This was done by applying the latest technology to assure that weapon performance conforms to standards associated with coupling of weapon-mount airframe or ground combat vehicles. To accomplish this purpose, the project required modifying the existing 6-DOF simulator to add active simulation in six degrees-of-freedom. These plans called for decoupling the six degrees-of-freedom, adding computer driven yaw and pitch motions, adding vibration input through the suspension actuators, automating the spring rate control, and installing a new hydraulic power supply. This report explains the different phases of the project in the order that they were implemented.

DESCRIPTION OF PASSIVE SIMULATOR

The passive 6-DOF simulator (fig. 1) was designed and built by the Franklin Institute Research Laboratories (FIRL) from five component systems: (1) the support and fork structure, (2) the yaw gimbal, (3) the pitch gimbal, (4) the triogonal actuator suspension, and (5) electronic and control consoles. The passive simulator supported a full-size helicopter hull, a lightweight tank cupola, or other vehicle sections weighing up to 9100 kg. The simulator was capable of absorbing the firing impulses of a 30-mm weapon. Hydraulic brakes helped in maintaining yaw position. The displacements of the system in response to the firing loads were in the three translational and the three rotational degrees-of-freedom; the displacements, however, were highly coupled.

The passive system had hand-operated controls for statically positioning a test vehicle suspended from the simulator at different yaw and pitch angles to set initial test conditions for off-axis firing of weapons. This permitted the weapon system to be counter-rotated to maintain projectile impact in the sand butt. However, the weapons could be fired at the initial preset angles only and not while the yaw and pitch angles were being altered.

The spring rate and damping characteristics of the passive simulator were determined by proper selection and adjustment of the pressures and volumes contained in the suspension actuator assemblies. Each of the suspension actuator assemblies consisted of a double-ended actuator having a total stroke of 22.9 cm, a bore of 15.3-cm diameter, and a rod of 7.6-cm diameter giving a piston working area of 136.8 cm^2 (piston area minus rod area).

Attached to the outer shell of the actuator chambers were two accumulators, one of which was piped to the top while the other was piped to the bottom chamber. Each accumulator had an oil-containing volume of 3.80 L and a nitrogen-containing volume of 3.85 L. The oil and nitrogen were separated by a movable piston, and a hand valve was inserted in the piping lines between the actuators and the accumulators to provide variable damping.

By proper selection of the variable parameters, the suspension system could be set to the desired spring rate, and damping ratios could be set by opening or closing the hand valves. Spring rates were obtained by the action of compressing a contained volume of nitrogen. Changes in spring rate were produced by changing the initial gas pressure, or volume, or both. Damping was obtained by directing the actuator fluid flow through a control orifice, and changing the size of the orifice varied the amount of damping. A complete description of the parameters affecting the spring rate and damping and the procedure for its adjustment are given in referenced technical manual.[2]

The time-consuming procedure for changing the spring rate and damping characteristics of the system involved the use of 12 hand-operated valves. When firing began, the spring rate increased along with the pressure in the hydraulic cylinders. The static spring rate initially set in the hydraulic cylinders changed as the dynamics of the system emerged. To achieve the full potential of the simulator, a method for maintaining a constant spring rate and damping coefficient was required.

Although the simulator absorbed the firing loads and responded to these loads in the three translational and the three rotational degrees-of-freedom, no external vibrations could be input to the weapon system. The mechanical characteristics were present, but the vibrational dynamic field environment in which the weapon system must operate could not be generated thereby negating the use of the passive simulator in its present state.

The requirement for testing weapons with two-axis stabilization systems indicated the need for activating the passive simulator. The test requirements warrant the use of a simulator with the capability of absorbing firing loads while the weapon system is being moved in combined yaw and pitch motions.

---

[2] "Helicopter Fuselage Mount Simulator," Technical Manual for Project No. C-2715, Contract DAAAF01-70-C-0406, Section III, November 1972, pp. 5-22.

Activation of the 6-DOF Simulator

Design Specifications

The passive 6-DOF simulator required several modifications before activation. The modifications are discussed in the approximate order in which they were accomplished. The activated simulator was to achieve the design objectives listed in table 1.

Modification of the Tiogonal Actuator System[3]

The activation of the 6-DOF suspension system is primarily a function of the control system which will be discussed later. The triogonal actuators were modified by adding sleeves to decrease the diameter of the cylinder bore and by adding new pistons to compensate for the reduced bore size. These changes were required to bring the flow rate at maximum velocity within the capabilities of the hydraulic pump units which resulted in more responsiveness between the suspension and the control systems.

Another change to the triogonal actuator assemblies involved the addition of hydraulic servovalves to control the hydraulic oil flow. Valve selection, maximum velocity, and area of actuator pistons were determined by the required flow rate. These changes were incorporated into the system in FY 75.

A detailed discussion of the design philosophy is given in ARTSD-SP-81001, which corresponds to this report.

Additional Hydraulic Power Supplies

The passive simulator was equipped with only a 30 L/min hydraulic power supply. Design calculations for the activated simulator are shown in table 2.

---

[3] Triogonal Actuator System. This is an assembly in which both the base and moving platforms are triangular in shape and connected at their vertices by six hydraulic actuators in a zigzag pattern. The entire assembly is an octahedron, that is, a separate frame composed of eight triangles.

Table 1. Design objectives for activating the passive simulator

Essential features	Weight or position	
	English	Metric
Suspended weight	300 - 18,000 lb	140 - 8,200 kg
Yaw displacement	+75° to -75°	+1.4 rad to -1.4 rad
Pitch displacement	+45° to -10°	0.8 rad to -0.18 rad
Spring rate		
x direction	250 to 250,000 lb/in.	44 to 44,000 kN/m
y direction	250 to 250,000 lb/in.	44 to 44,000 kN/m
z direction	250 to 250,000 lb/in.	44 to 44,000 kN/m
Normal position	Actuator midpoint	--
Pitch and yaw rates		
Helicopters	± 10° @ 0.3 Hz	± 0.18 rad @ 0.3 Hz
Combat vehicles	± 3° @ 3.5 Hz	± 0.054 rad @ 3.5 Hz
Firing impulse to be absorbed	140 lb-sec	620 N-sec
Vibrations	Typical of engine, tail rotor, main rotor	

Table 2. Required flow rates for full power simultaneous operation of all systems

Motion	Pump oil flow required for maximum performance (L/min)	
	Aircraft	Combat vehicle
Main pitch	810	—
Main yaw	90	--
6-DOF springs	830	120
Tail boom simulator	20	--
Turret pitch	--	480
Turret yaw (6-DOF)	--	900
Vibrators	70	70
Total for maximum performance	1,820	1,570

These flow rates are based on the use of accumulators in the lines that effectively reduce the actual pump flow to the above values.

The technical derivation and design philosophy for the selection of the hydraulic pump units are given in ARTSD-SP-81001.

The flow rate of 1,820 L/min is required for maximum performance with both motions and vibrations while simultaneously firing a 30-mm automatic weapon system. Because of funding limitations, only two 450 L/min pump units were installed. These are driven by two 190-kW motors (while this does create a limitation, all input requirements have been met for typical systems tested to date). Auxiliary pumps are used to raise the pressure to 700 kPa before the main pumps are activated.

The hydraulic pumps were plumbed into the system using high-pressure steel pipe 10 cm in diameter, which provided a working pressure of 21,000 kPa. The return pipes of the hydraulic system were diverted through four oil-to-air cooling units to reduce the temperature of the returning oil. The working fluid, MIL 5606 hydraulic oil, is then pumped into a 2.3 m^3 oil reserve tank. The hydraulic power supply system was installed by FIRL using local subcontracted millwrights.

Modifications to Control Panel

The control consoles for the passive and the activated 6-DOF simulator are shown in figures 2 and 3. The spring-rate setting for the passive 6-DOF simula-

tor required the hand adjustment of 12 valves. The procedure was time consuming, and a number of attempts to achieve the spring rate were required. The spring rate for the activated simulator is programmable and is automatically adjusted to the desired value. A unique closed-loop model following servo control system maintains the spring rate at the desired setting.

Several meters were added to the control panel that indicate the status of the hydraulic pump system. These meters indicate oil temperature, oil level, and oil filter condition. There are also controls for positioning the simulator and meters for indicating platform position. These include readouts such as length of actuator pistons, yaw and pitch position, and controls for manually setting spring rate, mass, yaw and pitch position, and damping values.

The control panels were modified and installed by FIRL personnel. The control panel cabinets also have plug-in electronic cards that are part of the closed-loop model following control circuits that maintain the constant spring rate of the actuators.

Automated Spring Rate Control

The hydraulic actuators of the 6-DOF simulator are regulated by an adaptive model following control system. This system allows each actuator to be programmed to simulate a specified spring-mass-damping model. The combination of each single-axis actuator system in the unique triogonal geometry provides an equivalent 6-DOF spring-mass-damping at the center of the simulator.

SINGLE AXIS CONTROL SYSTEM

Since the system is symmetrical, the control system for all six actuators is identical. Laplace transforms are used throughout the system to designate transfer functions. The linearized math model of a hydraulic actuator position control system, shown in figure 4, has a servovalve which controls fluid flow into a hydraulic piston with an attached effective mass (M). The control system was reduced to a simpler form in figure 5, and pertinent system functions are listed in equations 1 through 4 as follows:

$$\frac{sX}{Q} = \frac{\frac{1}{A}}{\frac{M}{K_H} S^2 \left(\frac{D}{K_H} + \frac{MC}{A^2}\right)S + 1 + \frac{DC}{A^2}} \tag{1}$$

$$\frac{X}{F} = \frac{\frac{C}{A}\left(\frac{A^2}{CK_H}s + 1\right)\left(\frac{s^2}{\omega^2} + \frac{2\xi}{\omega}s + 1\right)}{(Ms + Ds)\left(\frac{A}{K_H}s + \frac{C}{A}\right)\left(\frac{s^2}{\omega^2} + \frac{2\xi}{\omega}s + 1\right) + As\left(\frac{s^2}{\omega^2} + \frac{2\xi}{\omega}s + 1\right) + K_1K_2} \tag{2}$$

$$K_a = \frac{F}{X}\Big|_{\underset{s\to o}{Lim}} = \frac{K_1 K_2 A}{C} \quad \text{(actuator spring rate)} \tag{3}$$

$$K_v = \frac{K_1 K_2}{A\left(1 + \frac{DC}{A^2}\right)} \quad \text{(open loop position gain)} \tag{4}$$

From equations 3 and 4, we can relate the actuator spring rate to the open loop position gain if $\frac{DC}{A^2} << 1$.

For the 6-DOF simulator where

$$a = 68\ cm^2,\ C < \frac{18\ cm^5}{N \cdot sec} \quad \text{and} \quad D < \frac{37 N \cdot sec}{cm}$$

this inequality is true. Then the relationship between actuator spring rate and open loop position gain is

$$K_a = \frac{K_v A^2}{C} \tag{5}$$

Thus, by controlling the open loop position gain, the hydraulic actuator spring rate can be controlled which is the basis of the adaptive control system.

In the existing actuator control system, the open loop gain is set near the desired spring rate. Then the force applied to the actuator is measured and applied to an adaptive model of a spring-mass-damping system. The output of the model is compared to the existing actuator displacement, and this error signal is used to vary the forward loop position gain (K_v). A simplified block diagram of this system is shown in figure 6.

The only portion of this model not discussed yet is the force detection circuit. In the present system, the force (F) applied to the actuator is not measured directly.

Instead, the pressure drop across the actuator is measured which is equivalent to measuring the actuator-generated force (F_2). The force detection circuit operates on F_2 to produce energy equivalent to the applied force.

The operation of the force detection circuit is shown more clearly in figure 7 which contains a simplified version of figure 4. This figure shows that for $F_3 + F$ it is necessary that

$$G_f = \frac{F_3}{F_2} + \frac{F}{F_2} \tag{6}$$

However, from the block diagram we obtain

$$\frac{F_2}{F} = \frac{G_1 G_2}{1 + G_1 G_2} \tag{7}$$

Combining equations 6 and 7 for $F_3 + F$ we obtain

$$\frac{F_3}{F_2} = \frac{1 + G_1 G_2}{G_1 G_2} \tag{8}$$

Under conditions applicable to the existing actuators and substituting for G_1 and G_2 (fig. 4), we find that

$$\frac{F_3}{F_2} = \frac{M}{K_H} S^2 + \frac{MC}{A^2} S + 1 \tag{9}$$

This system is simulated by adding a second order lag function in the denominator with poles located at frequencies much higher than the zeros of equation 9.

The block diagram for the complete triogonal actuator control system is shown in figure 8.[4] The numbers in each block refer to the electronic boards identified on drawing 26D-105 that perform the functions of each block. The major inputs to each block are identified by board number and pin. Careful consideration of the block diagram reveals that it is essentially the same as that in figure 6. There have been many significant additions, and these are discussed below.

To slowly bring the actuator from its hydro off position (actuator pushed down) to its command position, two start-up circuits have been added. These are the zero error start-up and the servo start-up circuits. Both circuits reduce overall system gain and slowly increase it to its full value as the system reaches equilibrium.

The gain adjust circuit provides fixed gains of 1.45, 0.42, or 0.19 in the forward loop depending on the spring rate and damping set in the system. The spring rate and damping operate relays which select one of the three gains.

---

[4] This figure is directly related to FIRL drawing 26D-105, sheet 1, Triogonal Actuator Control System Electronics Schematic (Actuator 1).

The adaptive gain circuit varies the open loop gain of the system and provides a voltage output based on position input (2X) and integrated error input ($\frac{\varepsilon}{s}$) according to

$$V = 2X \cdot \left(1 + \frac{0.09\varepsilon}{s}\right) \tag{10}$$

Consider two cases

I $\quad \frac{\varepsilon}{s} = +10V$

$$V = 2X \cdot (1.9)$$

II $\quad \frac{\varepsilon}{s} = -10V$

$$V = 2X \cdot (0.1)$$

From these extremes the adaptive gain can vary over a 19 to 1 range.

Both the gain adjust and the adaptive gain circuits vary the system forward loop gain. The gain adjust circuit provides an adjustment of 7.63 to 1 and the adaptive gain circuit an adjustment of 19 to 1. As a result, the total forward loop gain can be varied over a 145 to 1 range. Since the forward loop gain is linearly proportional to the desired spring rate (see equation 5), the system spring rate can be varied over this same 145 to 1 ratio.

A valve-holding circuit has been added to account for steady state variations presented by solutions to the adaptive model. With a mass attached to the actuator, a steady state applied force will be sensed by the force detection circuit and the model will provide a position output (X_c). The actuator, however, will also try to follow its manual position command. The valve-holding circuit compensates for the resulting steady state position error.

The servovalve closed loop is a standard valve drive circuit. A dither circuit with f = 200 Hz has been added to reduce effects of stiction on system operation.

The force detection circuit is the same as explained previously with the following addition: The input to the system transfer function is normalized to prevent saturation and post multiplied to provide proper scaling. Consider equation 9 again in more general form

$$\frac{F_3}{F_2} = G \tag{11}$$

The actuator force (F_2) is normalized so that

$$N = \frac{F_2}{|F_2|} \tag{12}$$

After multiplying N by G, we postmultiply F_2 to obtain the desired result below

$$F_3 = N \cdot G \cdot |F_2| = F_2 G \tag{13}$$

The leakage coefficient of the hydraulic actuator is controlled by a valve attached to a potentiometer. The leakage coefficient is required by the force detection circuit. This coefficient is given by

$$C = \frac{Q}{\sqrt{P}} \tag{14}$$

where Q is the valve flow and P is the pressure drop across the load. This function is nonlinear and closely approaches

$$C = \frac{B}{\sqrt{P}} \tag{15}$$

where B is linearly related to the valve opening. Also, $p = F_2/A$ so that

$$C = \frac{B\sqrt{A}}{\sqrt{F_2}} \tag{16}$$

which is implemented by the leakage coefficient circuit.

The integrated error circuit was designed as shown in figure 3; however, a lead and lag network was added to improve system stability. The adaptive controller transfer function (H) is given by

$$H = \frac{4.93\ (1 + 2S)\ (1 + 0.0136s)}{s\ (1 + 0.0296s)} \tag{17}$$

The final circuit is the error limit comparator. This circuit provides a visual observation when the error exceeds a preset limit and can be used to stop weapon firing when the system error is too large.

The total system has been in operation for over two years and has proven extremely reliable. Some comments on its operation are as follows:

1. The achievable spring rates by the system are determined by the valve leakage coefficient and the load mass. This relationship is shown in figure 9.

2. Damping control in this system is difficult since it is dependent on the leakage coefficient and is given by

$$D = \frac{A^2}{C} \tag{18}$$

As a result, the leakage valve on each actuator must be manually adjusted to change damping.

3. The force detection circuit could be eliminated by direct measurement of forces applied to the actuator.

4. The contact relays in the gain adjust circuit would provide smoother operation if they were replaced by solid state relays.

5. Provision has been made in the circuit to input all critical parameters by computer rather than manually.

6. When the hydro ON button on the control console is selected, +28 VDC is supplied to the start up circuit of each actuator.

7. Actuator loads may be vibrated by applying a sinusoidal input to the system position command. Vibrations have been successfully applied out to frequencies of 20 Hz.

Installed Pitch and Yaw Motions

Pitch Gimbal

The pitch gimbal actuation system used on the passive simulator was found to be adequate for achieving the required performance of the activated simulator. An actuator force of 250 kN would be required for the Advanced Attack Helicopter under worst case conditions at the design acceleration of 0.62 rad/sec^2; the existing pitch actuator is capable of producing 480 kN of force. The existing structure was designed to withstand this hydraulic load. The flow rate requirement for the pitch servovalve was calculated at 1,270 L/min and is given in ARTSD-SP-81001. The existing hydraulic piping (sized for 30 L/min) and control wiring were completely changed to accommodate the new high rate of flow servovalve. In order to meet the flow requirement of 1,270 L/min, a Moog 79-400 valve with a model 73-233 electro-hydraulic servovalve as the pilot stage was installed. This valve combination is rated at 1,500 L/min at 6,900 kPa pressure drop. The valves were installed by FIRL personnel. The control wiring was also installed by FIRL personnel as explained in ARTSD-SP-81001.

Yaw Gimbal

The required yaw torque for the activated system is much greater than that of the passive simulator. In the passive system, a hydro/mechanical brake was available for holding the load under firing conditions. Because the activated system requires a fire-on-the-move capability, a brake system cannot be used.

Design calculations indicate that a yaw torque of 98 kNm was requried for the advanced attack helicopter at the design acceleration of 0.62 rad/sec^2. Since the hydraulic yaw motor on the passive system was rated at 14 kNm, it was inadequate for the activated system. The small capacity rotary actuator on the passive simulator was replaced by a larger one manufactured by Hagglund. The Hagglund model 8385 hydraulic motor has a rated capacity of 113 kNm at speeds from 0-16 rpm and does not require the use of rotary hydraulic joints in the pipelines leading to the valve or motor parts because of its unique construction. The hydraulic piping and electrical wiring were modified to accommodate the new high rate of flow servo system.

A Moog 79-060 valve with a 73-232 electro-hydraulic servovalve for the pilot stage was used to meet the flow requirement of 150 L/min. The above valve is rated at 225 L/min at 6,900 kPa pressure drop. The hydromechanical brake system used on the passive simulator is retained as a safety backup when the yaw servo is not energized. The brake system is rated at 410 kNm and is adequate for any contemplated loading.

The main yaw system has a torque capacity of 113 kNm. However, when the combat vehicle turret adaptor is mounted on the activated 6-DOF simulator, a peak torque of 270 kNm is required for high performance operation. The triogonal actuator system can be programmed to provide the high frequency yaw motion to the turret.

The technical details describing the detailed derivation of design and performance parameters of the main pitch system are covered in ARTSD-SP-81001.

Math Model

A mathematical model of the activated 6-DOF simulator was developed so that system characteristics could be thoroughly analyzed during the design phase. The math model was also used to derive the input data necessary to program the servo systems to (1) provide specified spring rates as measured at the platform, (2) eliminate the effects of gravity, because of the finite spring rate of the triogonal actuators as a result of variations in the geometry, and (3) derive the input signals necessary to produce the desired yaw and pitch motions.

The basic approach of the math model was to develop the equations necessary to relate forces and moments in one coordinate system to those in another and to relate velocities (linear and angular) of one system to another. The concept of impedance was introduced to describe the relationship between forces and moments

and the resultant velocities. With this method, the impedance seen at the mounting interface can be found in terms of the output impedance of the triogonal actuators. Hence, for a desired set of spring constants at the platform, the corresponding spring constants of the actuators can be found.

To determine origin displacement, a point in the gimbal system can be transformed into the platform system through the equation

$$X_{1P} = E\ (X_{3P})\ X_{1G} - r_p \tag{19}$$

where the angular tansformation is given by

$$E\ (X_3) = E_3\ (\phi)\ E_2\ (\Theta)\ E_1\ (\Psi) \tag{20}$$

and

$$E_2\ (\Psi) = \begin{bmatrix} \cos \Psi & \sin \Psi & 0 \\ -\sin \Psi & \cos \Psi & 0 \\ 0 & 0 & 1 \end{bmatrix} \tag{21}$$

$$E_2\ (\Theta) = \begin{bmatrix} \cos \Theta & 0 & -\sin \Theta \\ 0 & 1 & 0 \\ \sin \Theta & 0 & \cos \Theta \end{bmatrix} \tag{22}$$

$$E_3\ (\phi) = \begin{bmatrix} 1 & 0 & 0 \\ 0 & \cos \phi & \sin \phi \\ 0 & -\sin \phi & \cos \phi \end{bmatrix} \tag{23}$$

The displacement, r_p, is the vector from the origin of the gimbal system to the origin of the platform system, where it is measured.

The complete derivation and solution of the above equations is given in ARTSD-SP-81001.

The scalar actuator velocities are determined from the relative velocity of the platform system to the gimbal system, by first finding the vector velocities. For the n-th actuator, the vector velocity, in the gimbal coordinate is

$$\ell_{1G} = X_{1G} + E\ (X_{3P}) \cdot a \tag{24}$$

where

$X_{1G} = E\ (X_{3P})\ r_p$ is the location of the origin of the platform system in gimbal coordinates.

The further development of the scalar actuator velocity is given in ARTSD-TR-81001.

The impedance of a system is defined as the transformation which produces the system velocities in response to impressed forces and moments. Thus, in general,

$$\left(\frac{\dot{X}_1}{\dot{X}_2}\right) = Z\left(\frac{f}{m}\right) \tag{25}$$

with this definition of impedance seen looking into the platform coordinate system, as a result of the triogonal actuator impedances, is given by

$$\left(\frac{\dot{X}_{1P}}{\dot{X}_{2P}}\right) = Z_P\left(\frac{f}{m}\right)_p \tag{26}$$

The impedance matrix describing the actuators is

$$\dot{\ell} = Z_\ell f_\ell \tag{27}$$

where $\dot{\ell}$ and f_ℓ are the scalar lengths and forces in the actuators.

Further development of impedance is given in ARTSD-TR-81001.

The math model, an invaluable tool, was used extensively during the design, checkout, and operation of the activated 6-DOF simulator. The complete document describing the philosophy, the derivation, and the mathematics of the math model is in ARTSD-SP-81001.

Computer Implementation of Math Model

The math model equations developed for the simulator are nonlinear, but solutions for these equations are necessary so that the proper effective mass and spring rate setting for each individual actuator may be computed for variations in mounted weight, pitch angle, and yaw angle. It was determined that the most effective method for solving these equations was by a small general purpose digital computer. A Data General Nova 2/10 minicomputer with 16 K of memory was selected to perform the calculations. In addition, twenty-four 12-bit A/D channels and eight 12-bit D/A channels were purchased to allow the computer to update status of the simulator and to provide commands to the actuator control system in real time.

A description of the computer program implementing the math model and a listing of the program are included in ARTSD-SP-81001. The program is used presently in the off-line mode, calculating actuator effective masses and spring constants which are manually input to the simulator. The program has also been used in the on-line mode, however, operation of the program is too slow for real-time operation. For variable pitch angles of the system, the cycle time for one pass through the calculations is 0.57 cycles/sec. A hardware multiply and divide option for the computer will be purchased and will allow at least 50 cycles/sec through the model which is sufficient for real time applications.

TURRET ADAPTOR

The turret adaptor was designed and manufactured for testing the interaction between combat vehicles and the weapon systems mounted on them. The adaptor consists of a mounting plate and tube which is adjustable in the vertical direction. The tube is mounted in a roll gimbal ring which, in turn, is mounted on a pitch gimbal ring through trunnions and self-aligning ball joint type bearings. The pitch gimbal is mounted on the suspension ring through trunnions and self aligning ball-joint bearings similar to the gimbal trunnions. The turret adaptor is shown in figure 10.

The main suspension ring is designed to be attached directly to the clevis brackets of the 6-DOF suspension system rather than to the existing aircraft platform. This provides a greater available clearance to the floor and helps to keep the total moving weight at a minimum.

The connection between the adjustable tube and roll gimbal is a pair of taper wedge friction clamps designed to resist the torsional and thrust loads applied to it while permitting the axial adjustment of the turret in relation to the pitch axis within the 61 cm range provided.

The combat vehicle system is provided with its own actuator to provide desired pitch displacements. The actuator is controlled by the servo system. A Moog model 79-200 valve with a model 73-233 electro-hydraulic servo valve as the pilot stage is used to provide the flow requirement of 480 L/min. This valve combination is rated at 760 L/min at 6,900 kPa pressure drop. The actuator and valve combination also provides the variable spring rate in pitch. As noted in table 2, 480 L/min is required for moving a copula with a mass movement of inertia of 830 Nm^2 at 25 rad/sec^2 (maximum performance requirement). With the above valve combination, a flow of 280 L/min is available to provide spring characteristics. The system is not flow limited at any combination of firing forces and spring rates within the system operating range.

The triogonal actuator suspension system will be programmed to provide the high frequency yaw motion to the turret adaptor while retaining its effectiveness as a spring simulator.

Detailed design parameters and derivation of equation for the turret adaptor are given in ARTSD-SP-81001.

EXPANSION OF DATA ACQUISITION AND REDUCTION SYSTEM

During FY 69, ARRADCOM contracted with Honeywell for an automated data acquisition and reduction system. Although the system as delivered and installed did function, it was found to be lacking in several design areas and limited in capability. The original acquisition system included five charge amplifiers, 12 bridge completion models, 12-dc amplifiers, one thermocouple and millivolt module, and an analog tape deck with 14 recording heads.

Design inadequacies inlcuded:

1. Poor placement of equipment
2. Patch board confusion and limited bus capability
3. Inability for one person to balance a bridge circuit
4. Excessive length of transducer cables
5. High noise levels on strain channels
6. Limited calibration capabilities

The updating and expansion of the original data acquisition system was undertaken during this phase of the project. This expansion would provide more flexibility in patch-bay hookup and also provide more analog recording capability.

The major procurement effort was the expansion from 14 to 28 channels of recording capability. The activation of the 6-DOF required more than the original 14 data channels to handle the increased data requirements, i.e., pitch, yaw and roll of the hull, 3-axis forces, and 3-axis displacements. These measurements are required so that the motion of the vehicle attached to the simulator can be described as it is moved in space. Therefore, 28 track-heads for the analog tape recorder were purchased along with 14 record boards, 14 current driver boards with 14 record boards, and a dc power supply to handle the increased current demand. These components were installed and the tape recording system was recalibrated to permit 28-channel operation.

The major labor effort involved the rearrangement of the data acquisition components and the subsequent rewiring of all the patch panels. In addition, more signal conditioning was purchased, which also had to be wired into patch panels.

A "straight-through" design was achieved by rewiring the patch panels. This was done by directly wiring the first of each element of the tape transport to one another in the following sequence: transducer, bridge module, amplifier, channel. External patch cords are used only when a defective unit is bypassed and replaced with another unit.

The major rearrangement consisted of interchanging the input bay and the output and record-input bay. Previously, the low-level signals entered from the north end of the data acquisition room (fig. 11) and traveled to the input bay on the south end of the room. At this point, the appropriate signal conditioning was selected, the signal amplified and sent back to the north end of the room where the output bay and record input was located. When data was being analyzed in real time, it was sent across the room again to the adjacent data reduction room. Thus, data would cross the room three times.

To eliminate this problem, the input bay was moved to the far north end of the room. The calibrator and signal conditioning amplifiers were moved adjacent

to the input bay. The amplifier output monitoring meters were moved adjacent to the bridge balancing unit to enable one person to balance the bridge by observing the output meters (this was impossible before because of the location). These signals, then, are available at the output bay where they may go directly to the tape recorder or to the data reduction room for real time analysis.

CONCLUSIONS

The activated 6-DOF simulator provides the Army with an excellent tool for testing weapon systems under live firing conditions. The simulator can input vibrations and pitch or yaw motions to mounted system while they are firing. The exact motion spectrum that can be input to a mounted system is dependent on the mass of inertia of the mounted system. The system performance with only the mounting platform attached for a sinusoidal command is as follows: (1) pitch, 20°/sec, (2) yaw, 10°/sec, and (3) frequency range, 0.5-3.0 Hz. This repsonse is degraded somewhat as increasing mass is mounted on the simulator. At lower input frequencies, the velocity is reduced, but the sinusoidal amplitude can be increased to a maximum of 25° for pitch and 65° for yaw.

The vibration spectrum that can be supplied to the system with only the mounting platform attached is given as follows:

Input	Frequency range
15.0 cm/sec	0.5-5.0 Hz
0.5 g	6.0-18 Hz

From 5 Hz to 6 Hz, reduced amplitude must be supplied by the actuator system, since the simulator suspension tower has a resonance at 5.5 Hz.

The vibration system has been used successfully to test the vibration response of various weapons and weapon systems. For example, the response and accuracy of the 30-mm Rarden weapon was measured for vibration inputs from 1.0 to 7.0 Hz. Also, the barrel response in a nonfiring mode was measured from 0.5 to 18.0 Hz.

In addition, the simulator spring rates can be programmed so that mounted systems will respond to firing impulses in the same manner as they do in the field. The achievable spring rates are again determined by the mass of the mounted system and are described in figure 9. The determination of the spring rate setting is made by matching the resonant spring rate of the system on the simulator to the equivalent resonant frequency of the system in the field.

The simulator is now an effective mechanism for testing weapons or weapon systems under controlled, repeatable conditions. It provides the Army with a test method between the costly and time-consuming extreme of field testing and the oversimplified firing tests from hard mounts.

Figure 1. Passive simulator with UH-1B helicopter suspended from mounting platform

Figure 2. Passive 6-DOF simulator control console

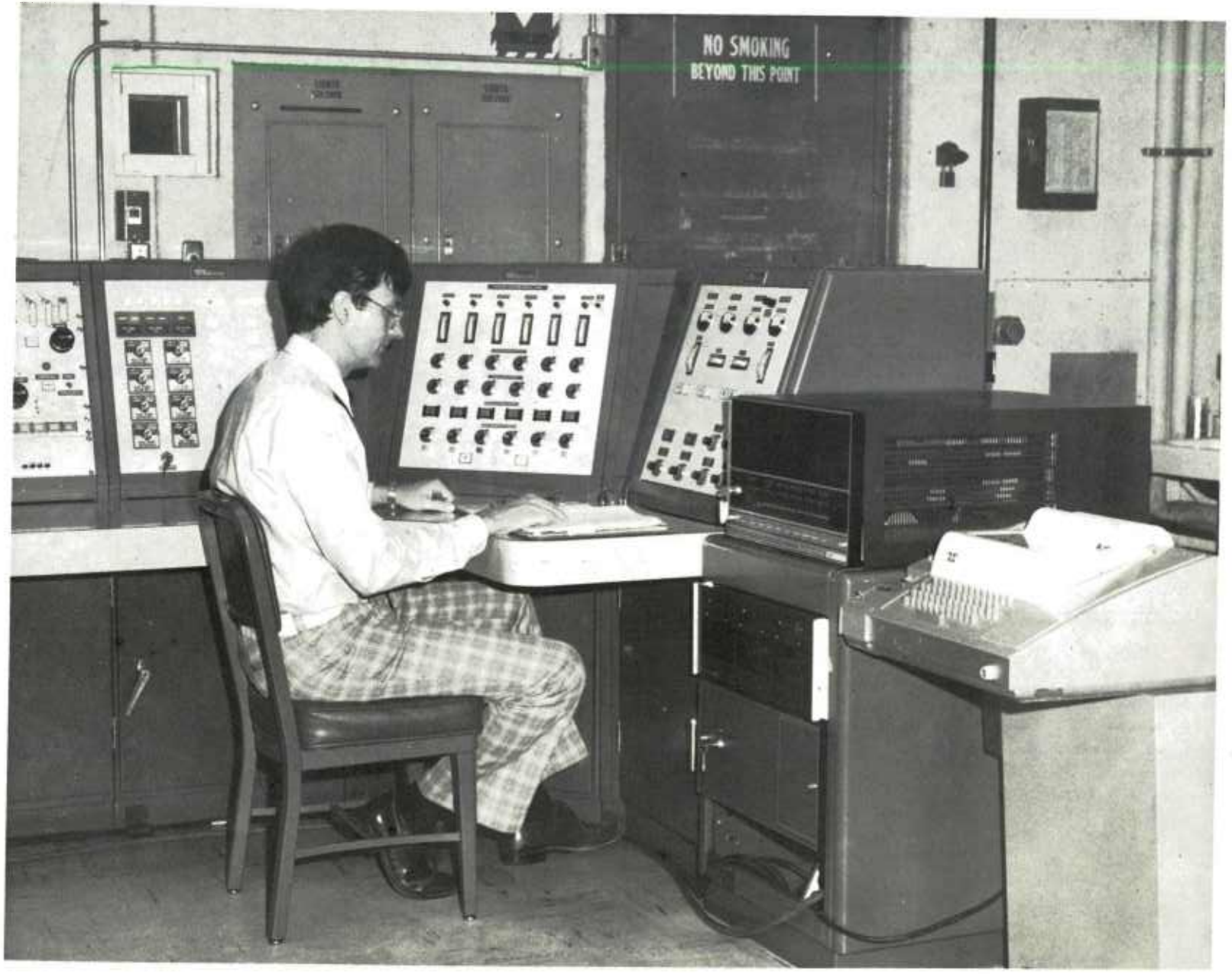

Figure 3. Active 6-DOF simulator control console

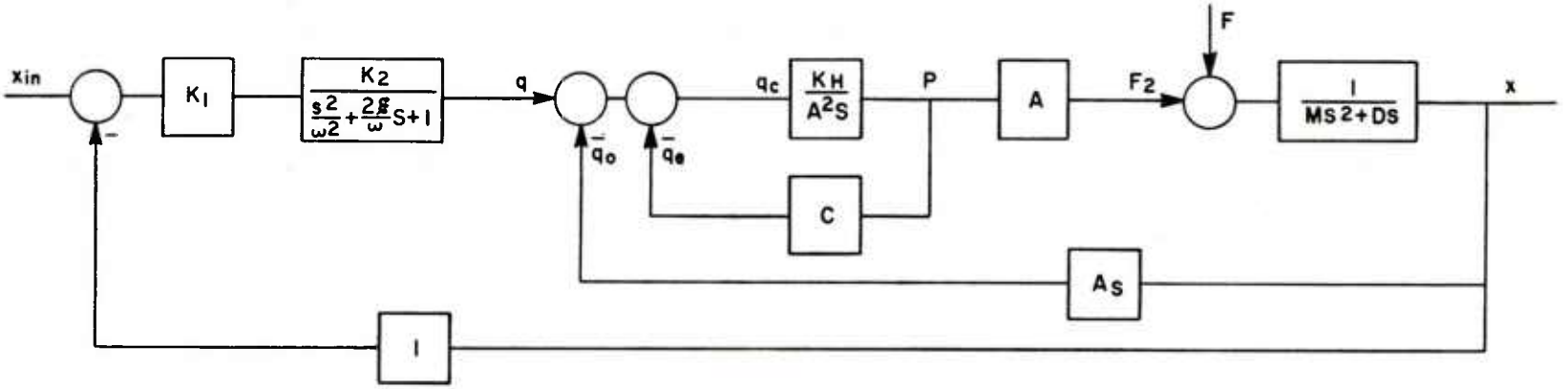

M - Actuator Load

D - Actuator Damping Coefficient

A - Piston Area

K_H - Actuator Hydraulic Stiffness

K_1, K_2 - System Gains

C - Hydraulic Valve Leakage

q - Servo Flow = $q_o + q_e + q_c$

q_o - Incompressible Flow

q_e - Leakage Component

q_c - Compressible Flow

ω - Servovalve Natural Frequency

ξ - Servovalve Damping Ratio

Figure 4. Linearized math model of a hydraulic actuator position control system

TRIOGONAL ACTUATOR SYSTEM

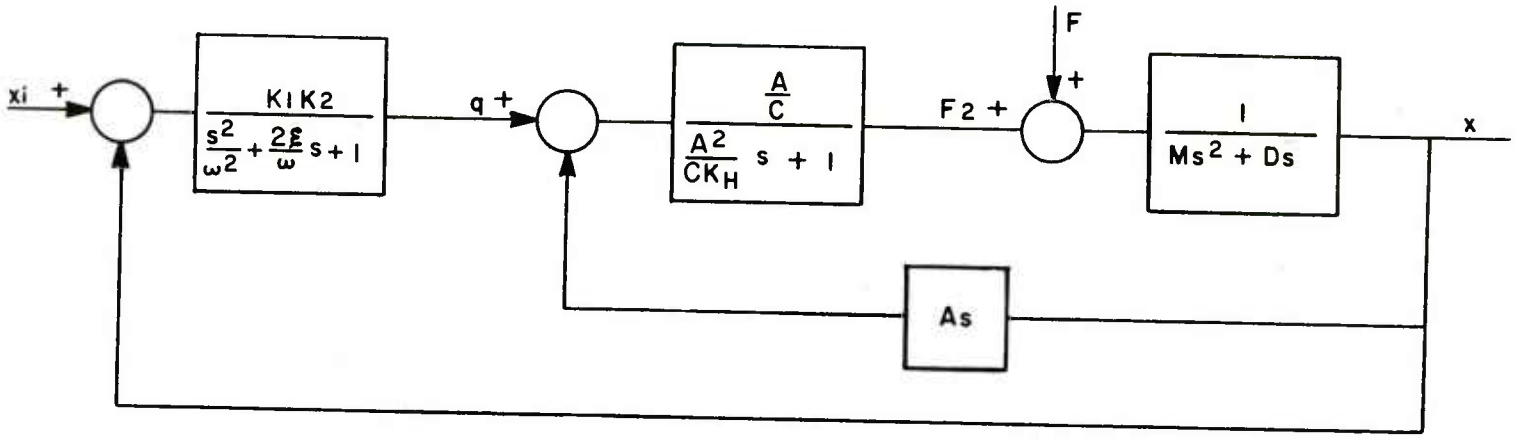

FOR OPEN LOOP POSITION

$$\frac{sX}{Q} = \frac{\frac{1}{A}}{\frac{M}{K_H}S^2 + \left(\frac{D}{K_H} + \frac{MC}{A^2}\right)S + 1 + \frac{DC}{A^2}} \qquad (1)$$

$$\frac{X}{F} = \frac{\frac{C}{A}\left(\frac{A^2}{CK_H}s + 1\right)\left(\frac{s^2}{\omega^2} + \frac{2\xi}{\omega}s + 1\right)}{(Ms + Ds)\left(\frac{A}{K_H}s + \frac{C}{A}\right)\left(\frac{s^2}{\omega^2} + \frac{2\xi}{\omega}s + 1\right) + As\left(\frac{s^2}{\omega^2} + \frac{2\xi}{\omega}s + 1\right) + K_1 K_2} \qquad (2)$$

$$K_a = \left.\frac{F}{X}\right|_{\substack{\text{Lim} \\ S \to 0}} = \frac{K_1 K_2 A}{C} \quad \text{(Actuator Spring Rate)} \qquad (3)$$

$$K_v = \frac{K_1 K_2}{A\left(1 + \frac{DC}{A^2}\right)} \quad \text{(Open Loop Position Gain)} \qquad (4)$$

Figure 5. Simplified form of the control system with pertinent system equations

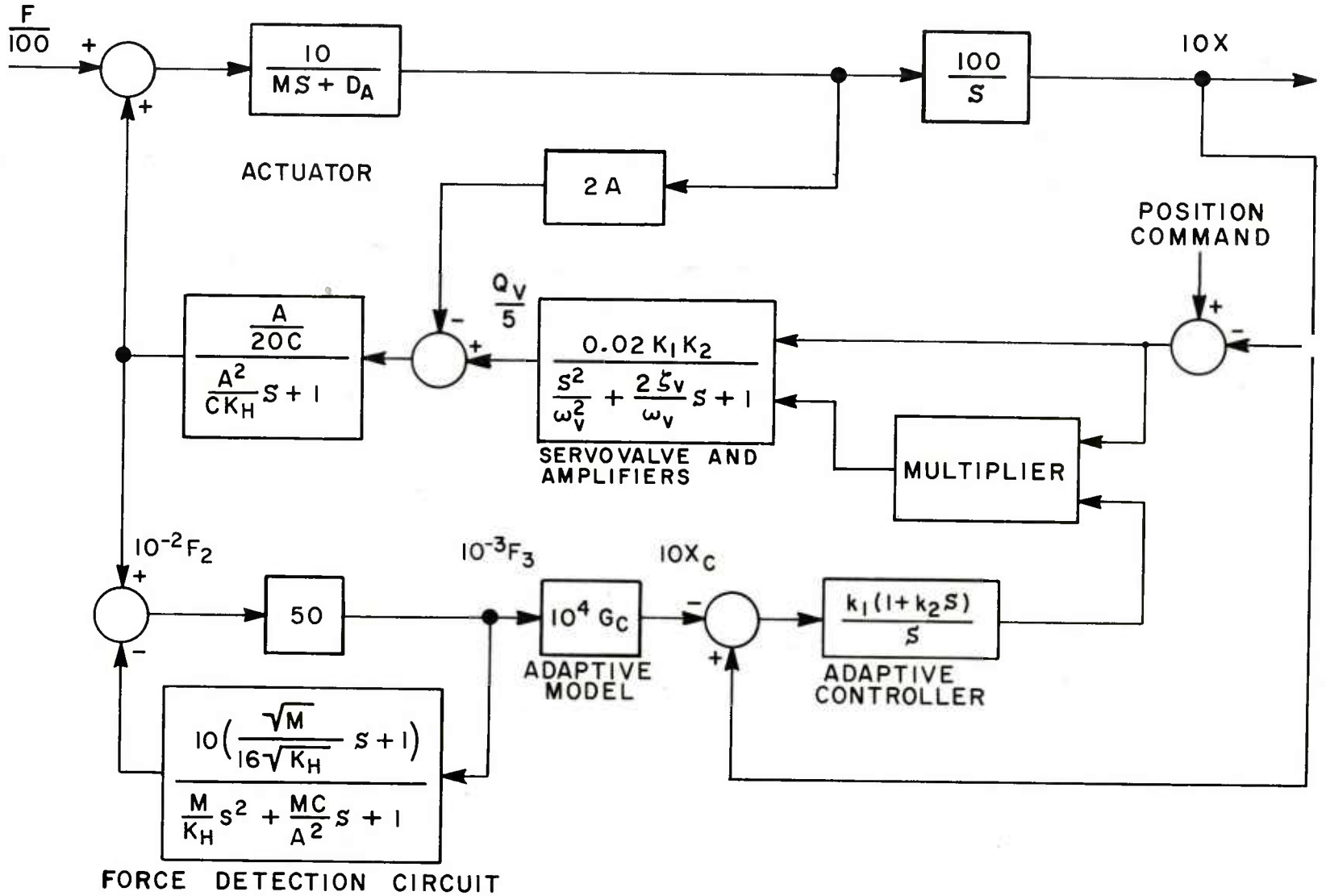

Figure 6. Simplified block diagram of adaptive spring rate control system

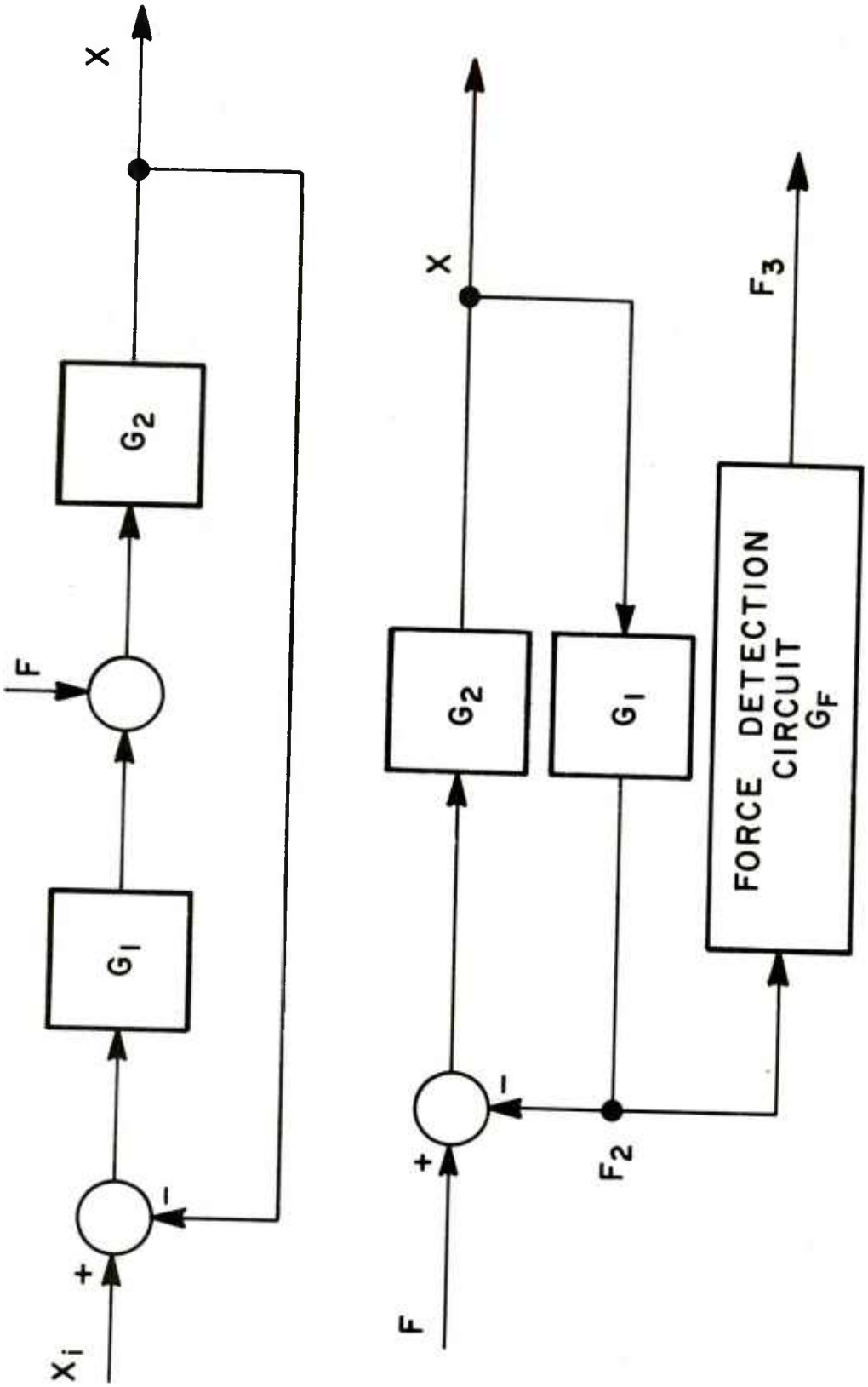

Figure 7. Block diagram of force detection circuit

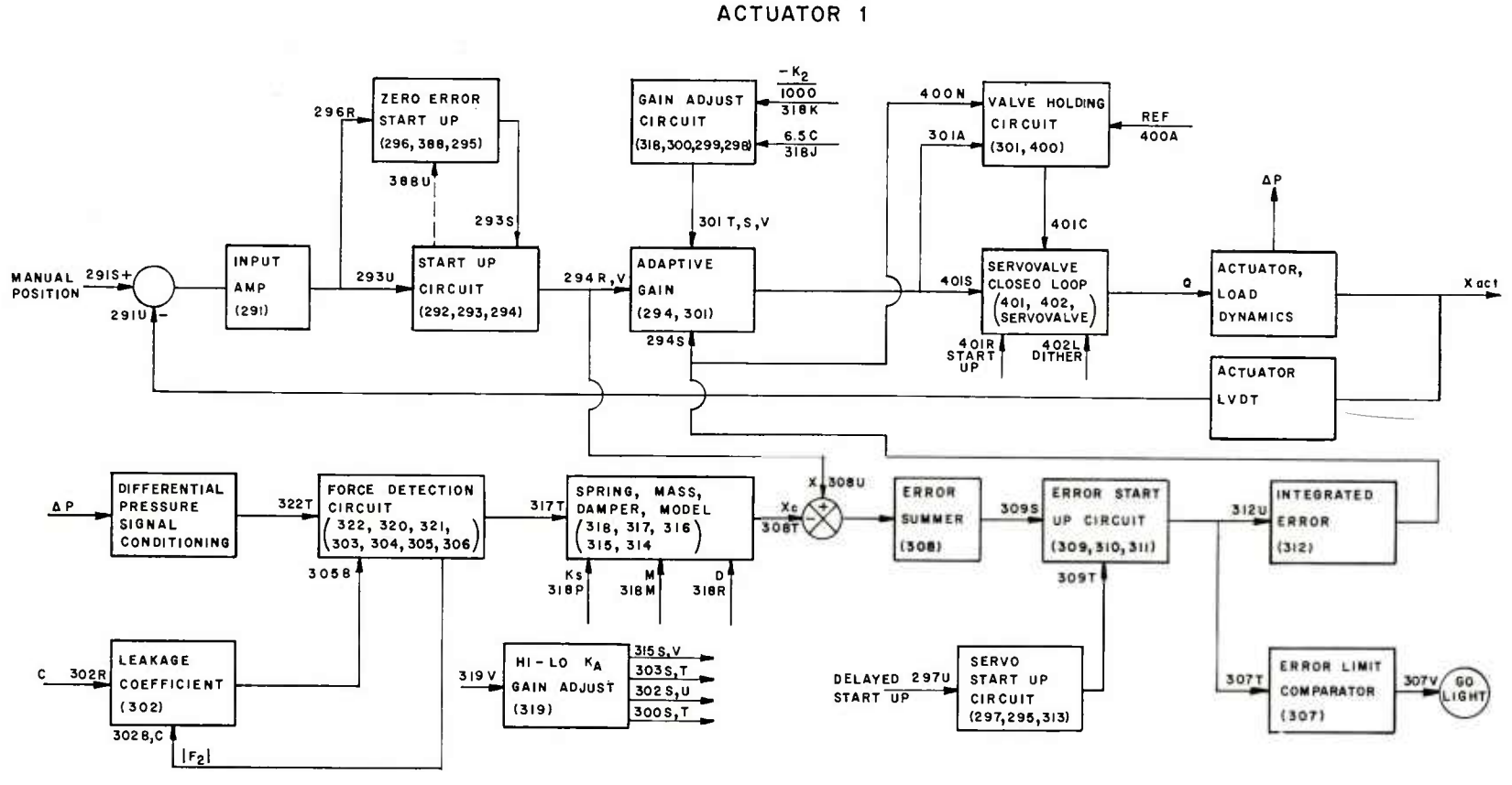

Figure 8. Block diagram of complete triogonal actuator system

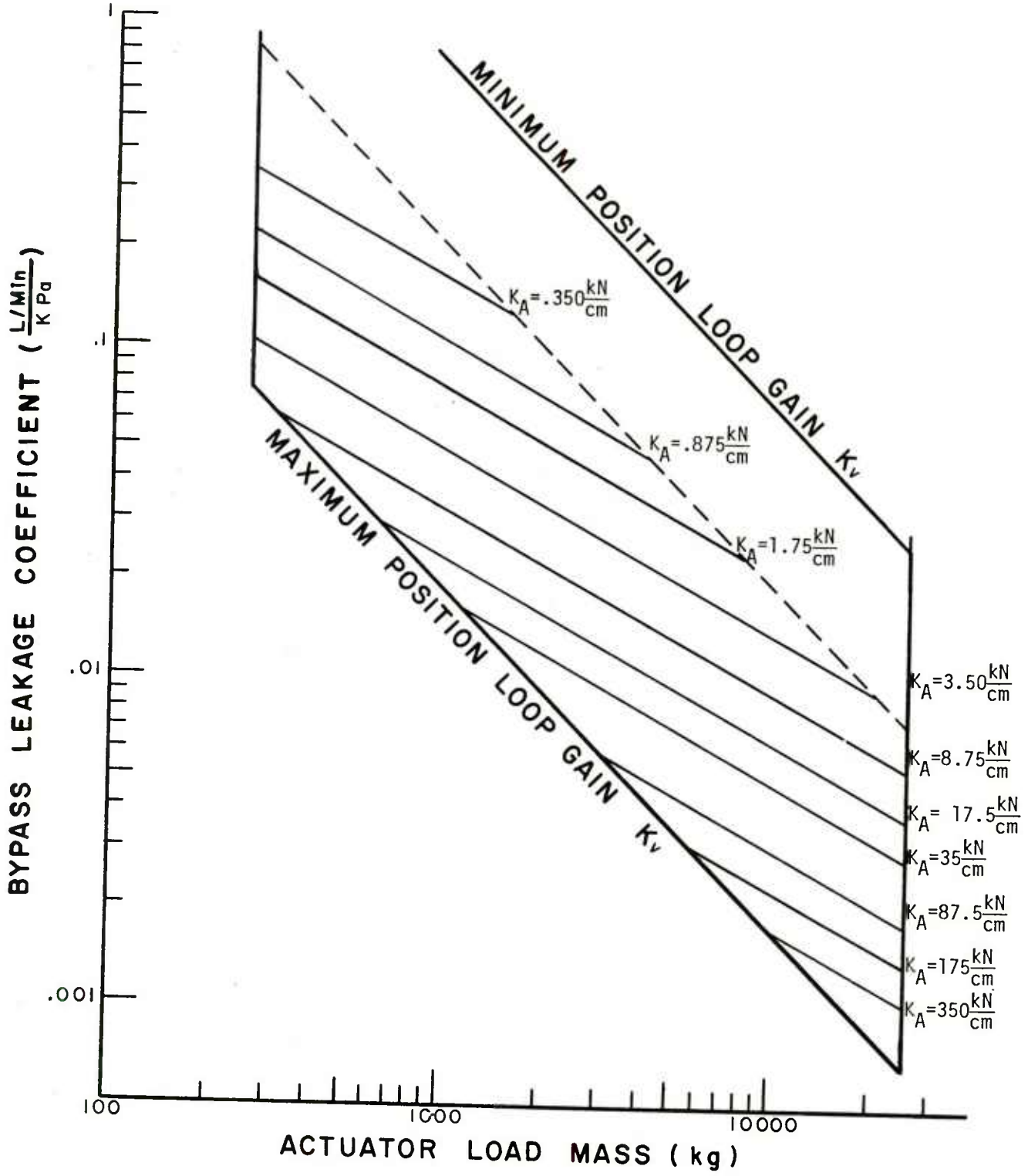

Figure 9. Allowable spring rates as limited by servovalve leakage and load mass

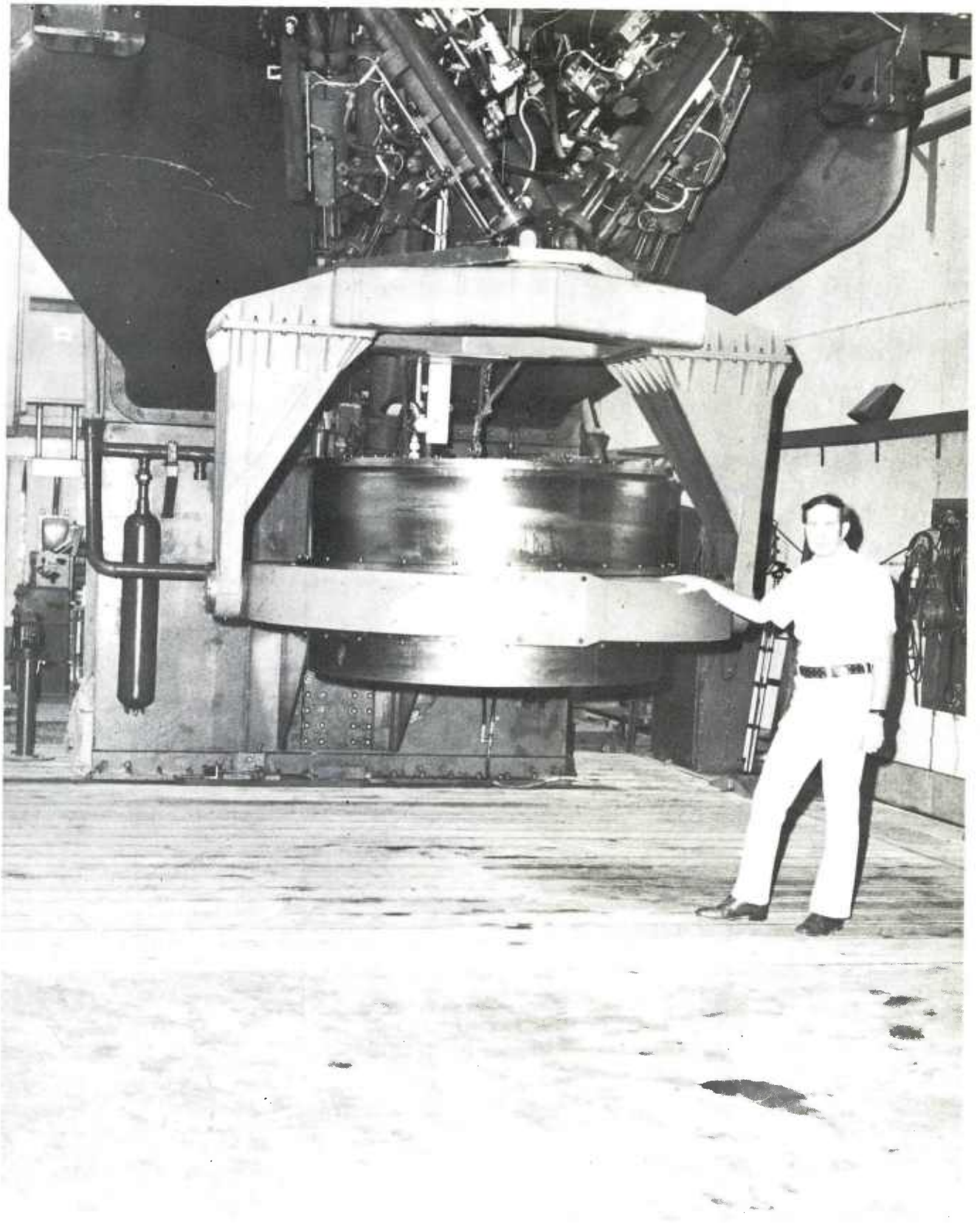

Figure 10. Turret adaptor suspended from 6-DOF simulator

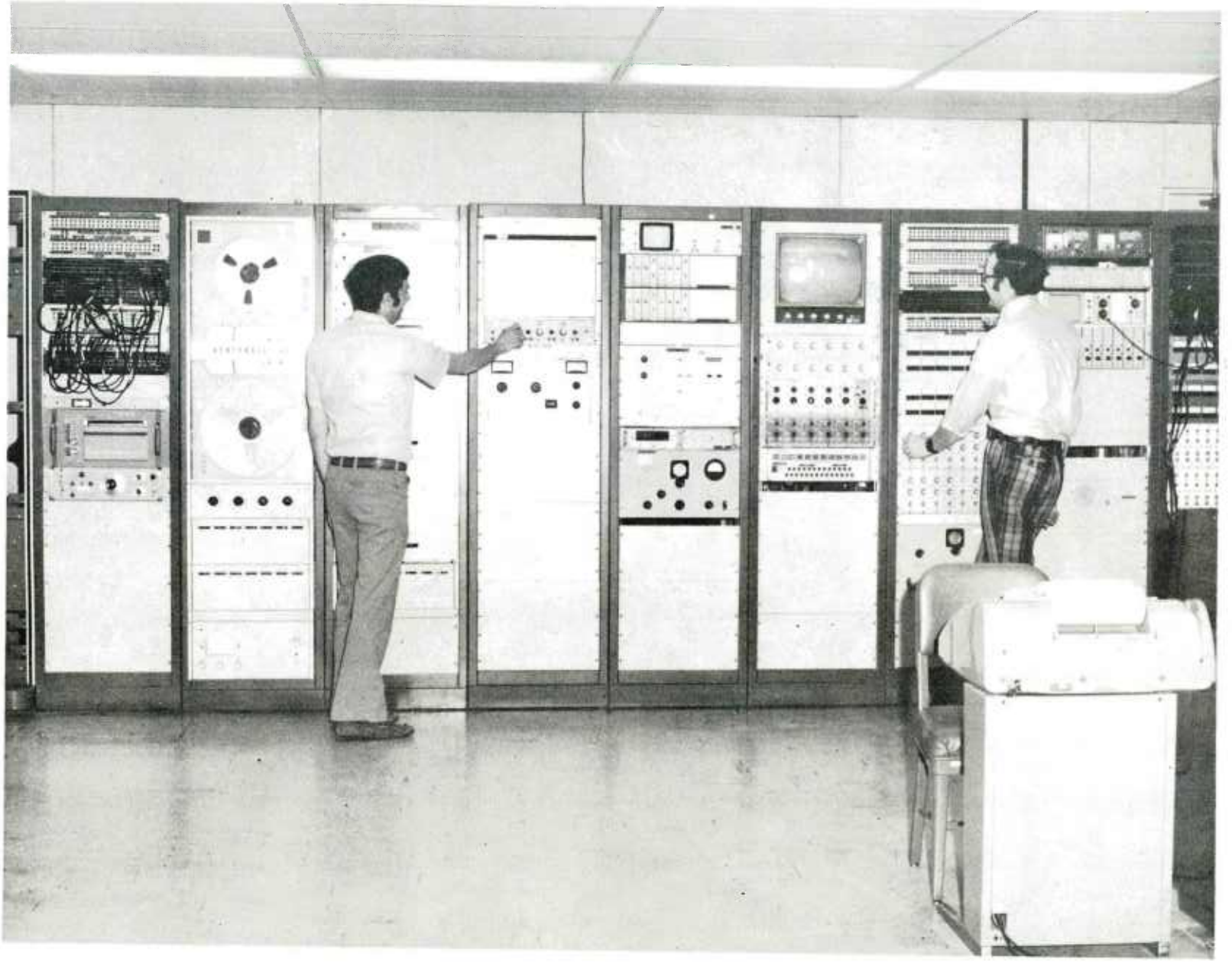

Figure 11. Data acquisition room after expansion to support 6-DOF simulator

DISTRIBUTION LIST

Commander
U.S. Army Armament Research
and Development Command
ATTN: DRDAR-SC
DRDAR-SCA (4)
DRDAR-SCF (2)
DRDAR-SCS (2)
DRDAR-TSE-E
DRDAR-TSS (5)
DRDAR-GCL
Dover, NJ 07801

Administrator
Defense Technical Information Center
ATTN: Accessions Division (12)
Cameron Station
Alexandria, VA 22314

Director
U.S. Army Materiel Systems
Analysis Activity
ATTN: DRXSY-MP
DRXSY-O
Aberdeen Proving Ground, MD 21005

Commander/Director
Chemical Systems Laboratory
U.S. Army Armament Research
and Development Command
ATTN: DRDAR-CLJ-L
DRDAR-CLB-PA
APG, Edgewood Area, MD 21010

Director
Ballistics Research Laboratory
U.S. Army Armament Research
and Development Command
ATTN: DRDAR-TSB-S
Aberdeen Proving Ground, MD 21005

Chief
Benet Weapons Laboratory, LCWSL
U.S. Army Armament Research
and Development Command
ATTN: DRDAR-LCB-TL
Watervliet, NY 12189

Commander
U.S. Army Armament Materiel
  Readiness Command
ATTN: DRSAR-LEP-L
      DRSAR-IRW
Rock Island, IL 61299

Director
U.S. Army TRADOC Systems
  Analysis Activity
ATTN: ATAA-SL
White Sands Missile Range, NM 88002

Human Engineering Laboratories
  Liaison Office
ATTN: Len Wascher
220 7th Street
Charlottesville, VA 22901

Project Manager, Cobra
ATTN: DRCPM-CO-TM
4300 Goodfellow Blvd.
St. Louis, MO 63120

Program Manager
Advanced Attack Helicopter
ATTN: DRCPM-AAH-TM
4300 Goodfellow Blvd.
St. Louis, MO 63120

Department of the Army
Program Manager
Fighting Vehicle Systems
ATTN: DRCPM-FVA
      DRCPM-FVS-SE
Warren, MI 48090

Commander
Rock Island Arsenal
ATTN: SARRI-EN
      SARRI-ADL (2)
Rock Island, IL 61299

Office of the Deputy Undersecretary of
  Defense Research and Engineering
Pentagon Room 3D1098
Washington, DC 20301

Commander
Headquarters, Army Materiel Development
and Readiness Command
ATTN: DRCDE
DRCIRD
5001 Eisenhower Avenue
Alexandria, VA 22333

Commander
Combined Arms Center
ATTN: ATCA-COF
Ft. Leavenworth, KS 66048

Commanding General
Training and Doctrine Command
ATTN: Library, Bldg 133
Ft. Monroe, VA 23651

Commander
Army Tank Automotive Research
and Development Command
ATTN: DRDTA-UL, Library
Warren, MI 48090

Commandant
U.S. Army Aviation Center
P.O. Box 0
ATTN: USAAVNT, Library
Ft. Rucker, AL 36362

Commander
Harry Diamond Laboratory
2800 Powder Mill Road
ATTN: DELHD-PP
Adelphi, MD 20783

Commander
U.S. Army Aviation Research
and Development Command
P.O. Box 209
ATTN: DRDAV-EVW
St. Louis, MO 63166

Headquarters
U.S. Army Research and
TechnicalLaboratory
Ames Research Center
ATTN: DAVDL-AS
Moffett Field, CA 94035

Commander
Naval Weapons Center
ATTN: Code 3176, Technical Library
China Lake, CA 03555

Department of the Navy
Naval Air Systems Command
ATTN: Code 5323D, Technical Library
Washington, DC 20361

Commander
Naval Surface Weapons Center
ATTN: Code G22, Technical Library
Dahlgren, VA 22448

Commander
Air Force Armament Laboratory
ATTN: Technical Library
Eglin Air Force Base, FL 32548